Mechanistic insight into the improved photocatalytic degradation of dyes for an ultrathin coating of SiO_2 on TiO_2 (P25) nanoparticles

Benz, Dominik; Van Bui, Hao; Hintzen, Hubertus T.; Kreutzer, Michiel T.; van Ommen, J. Ruud

DOI
10.1016/j.ceja.2022.100288

Publication date
2022

Document Version
Final published version

Published in
Chemical Engineering Journal Advances

Chemical Engineering Journal Advances 10 (2022) 100288

Contents lists available at ScienceDirect

Chemical Engineering Journal Advances

journal homepage: www.sciencedirect.com/journal/chemical-engineering-journal-advances

Mechanistic insight into the improved photocatalytic degradation of dyes for an ultrathin coating of SiO_2 on TiO_2 (P25) nanoparticles

Dominik Benz [a], Hao Van Bui [b], Hubertus T. Hintzen [c], Michiel T. Kreutzer [d], J. Ruud van Ommen [a,*]

[a] Department of Chemical Engineering, Delft University of Technology, Van der Maasweg 9, 2629 HZ Delft, Netherlands
[b] Faculty of Materials Science and Engineering, Phenikaa University, Yen Nghia Ward, Ha-Dong District, Hanoi, 12116, Vietnam
[c] Fundamental Aspects of Materials and Energy, Delft University of Technology, Mekelweg 15, 2629 JB Delft, Netherlands
[d] Faculty of Architecture, Delft University of Technology, Julianalaan 134, 2628 BL Delft, Netherlands

ARTICLE INFO

Keywords:
Photocatalysis
Atomic layer deposition
Dye degradation
Mechanism
SiO_2 on TiO_2

ABSTRACT

The photocatalytic mechanism of TiO_2 (P25) nanoparticles coated with SiO_2 (SiO_2:TiO_2) by atomic layer deposition was investigated. The deposition of SiO_2 on TiO_2 not only gives a photocatalytic improvement for the degradation of both Rhodamine B (3.6–fold) and Acid Blue 9 (3–fold). SiO_2 deposition also changes the mechanism from direct oxidation of the pollutant at the surface of TiO_2 to a predominantly OH* radical based degradation of the pollutants originating from SiO_2:TiO_2. Low SiO_2 loadings on TiO_2, where the coating is incomplete, improve the OH* radicals generation due to the higher number of acidic Si–OH groups combined with the facilitated charge separation at the TiO_2–SiO_2 interface. As a consequence of incomplete coverage, the TiO_2 surface remains accessible, which allows both the oxidation and reduction reactions at the SiO_2:TiO_2 surface. On the other hand, high loading of SiO_2 (>3 wt.% Si) results in photocatalytic suppression due to the coverage of TiO_2 surface by SiO_2. The degradation of differently charged dyes on the SiO_2:TiO_2 surface demonstrates the independence of the adsorption properties on the photocatalytic improvement. Simultaneous degradation of two dyes demonstrated the advantage of SiO_2:TiO_2 being less selective and, therefore, better suited for general water purification.

1. Introduction

Photocatalysis undoubtedly has excellent potential for several environmental applications, such as air purification and water cleaning. Since the first paper by Fujishima and Honda [1] almost 50 years ago, the field has progressed substantially. However, further significant steps are required to come to the broad implementation of this technology. For the commonly used photocatalyst TiO_2, numerous studies have investigated the photocatalytic mechanism [2–11]. Nevertheless, improved photocatalysts based on modifications of TiO_2 are often still lacking a clear description of the photocatalytic mechanism. The lack of insight hampers the rational design of high-performance photocatalysts, where the combination of multiple materials could lead to significant activity improvement.

The photocatalytic activity is commonly improved by adding materials onto the surface, enhancing one or more properties influencing the photocatalytic mechanism [12–17]. In heterogeneous photocatalysis for water treatment, four different steps are essential for a reaction: 1) adsorption of reactants to the surface, 2) light absorption of the catalyst leading to excitation of an electron from the valence band (VB) to the conduction band (CB) 3) redox reactions of the reactants (pollutant, H_2O or O_2) on the surface to directly degrade pollutants or generate reactive oxygen species (ROS) and 4) desorption of the reactant from the surface. Upon light absorption with an energy higher than the bandgap, an electron (e^-) is excited to the conduction band, leaving a hole (h^+) back in the valence band. Excited electrons can reduce the dissolved O_2 in the water to a superoxide radical $O_2{}^{*-}$, further reacting to OH* radicals and subsequently attacking and degrading the pollutant. Moreover, holes in the VB can either oxidize the pollutant directly or react with water to form hydroxyl radicals OH*, which subsequently attack the pollutant [18, 19]. In order to improve the performance of a photocatalyst, different strategies can be applied to optimize the properties involved in each step: 1) Increase the adsorption of the reactants to reduce mass transfer limitations, 2) absorb more light to generate more charge

* Corresponding author.
E-mail addresses: d.benz@tudelft.nl (D. Benz), j.r.vanommen@tudelft.nl (J.R. van Ommen).

https://doi.org/10.1016/j.ceja.2022.100288
Received 14 October 2021; Received in revised form 7 March 2022; Accepted 15 March 2022
Available online 16 March 2022

carriers or utilize the light better by preventing electron-hole recombination, 3) improve the formation of reactive oxygen species (OH*, O_2^{*-}) to degrade pollutants faster, and 4) enhance the desorption of products to prevent surface poisoning [20–23].

The seek for cheaper materials drew research away from noble metals and towards metal oxides. Photocatalysts containing both SiO_2 and TiO_2 were investigated widely in recent research. However, SiO_2 was mostly used as a substrate where TiO_2 was deposited onto. It is believed that SiO_2, due to its electronic properties, will block the photocatalytic activity [24–28]. Reports indicate that by using SiO_2 as a substrate, the adsorption of pollutants increases due to a change in the surface charge/zeta potential leading to an improvement in the photocatalytic activity [24, 25]. Only recently, studies of core/shell particles with TiO_2 and SiO_2 have elaborated on the photocatalytic activity of degrading organic pollutants [29–37]. Very low loadings of SiO_2 on TiO_2 are needed to observe an improvement in the photocatalytic activity. The reasons for the enhancement are ascribed to enhanced adsorption [29, 30, 38] and better charge transfer/ improved charge separation [39–41] or better desorption of the degradation products [31, 32]. However, an overall understanding with a clear insight into the predominant photocatalytic reaction pathway is still lacking.

This paper elucidates the photocatalytic mechanism of SiO_2 coated TiO_2 by evaluating the fundamental steps in photocatalysis for TiO_2 compared to SiO_2:TiO_2. Applying the findings from our previous work and PhD research [17, 42] atomic layer deposition allowed us to build up SiO_2 layer by layer onto TiO_2. The thus obtained materials will serve us to clarify the predominant photocatalytic pathways. By comparing the degradation behavior of two oppositely charged pollutants, we elaborate on the importance of adsorption on the surface. Sacrificial agents and simultaneous degradation of two oppositely charged dye molecules gave insight into predominant photocatalytic pathways for radical generation. For this purpose, we employ atomic layer deposition (ALD) to deposit ultra-thin layers of SiO_2 onto TiO_2 particles to obtain a model catalyst where we are able to investigate the photocatalytic mechanism in detail. This study will open up the door for further developments of novel multi-component materials. Different functionalities linked to subsequent mechanisms steps could be added to improve the catalytic activity further.

2. Experimental section

2.1. Materials synthesis

TiO_2 (P25) nanoparticles (mean diameter ~21 nm, specific surface area of ~54 m^2g^{-1} measured by BET) were purchased from Evonik Industries (Hanau, Germany). The powder was sieved prior to the ALD experiments with a 250 μm sieve to break or exclude larger agglomerates. Silicon tetrachloride ($SiCl_4$) was purchased from Sigma-Aldrich and stored in a stainless-steel bubbler for mounting into the ALD setup. Acid Blue 9 (AB9), Rhodamine B (RhB), Methanol, and DMSO were purchased from Sigma Aldrich and were used without further purification.

Silicon dioxide was deposited on the TiO_2 particles on a homebuilt ALD setup in a fluidized bed under atmospheric pressure based on a setup described elsewhere [43, 44]. In brief, the TiO_2 powder was placed in a quartz glass column (diameter 26 mm, height 500 mm), which was then placed on a vertical vibration table (Paja 40/40–24) to assist fluidization. SiO_2 was deposited using $SiCl_4$ and H_2O as precursors, which both were kept at room temperature in stainless steel bubblers. The reactor was heated to 100 °C by an IR lamp, and a temperature feedback controller was placed inside the powder bed throughout the deposition process. Different SiO_2 loadings were produced by applying up to 40 cycles using 30 s $SiCl_4$ exposure and a 30 s water pulse. The precursors were carried to the reactor by a flow of nitrogen (0.5 L/min) and the pulses were separated by purging steps of nitrogen for 3 min and 8 min, respectively. Afterward, the samples were calcined at 500 °C for 2 h in air in a Neytech Vulcan Benchtop furnace.

2.2. Materials characterization

For the ICP-OES analysis, approximately 30 mg of sample was destructed in 4.5 ml 30% HCl + 1.5 ml 65% HNO_3 + 0.2 ml 40% HF acid mixture using a microwave. The destruction time in the microwave was 60 min. After the destruction, the samples were diluted to 50 ml with Milli-Q and analyzed with ICP-OES 5300DV. For Ti analysis, the samples were also diluted 20 times.

TEM micrographs were acquired from a JEOL JEM1400 transmission electron microscope at 120 kV. As-deposited TiO_2-SiO_2 nanoparticles were suspended in ethanol and transferred to Cu transmission electron microscopy grids (3.05 mm in diameter, Quantifoil).

X-ray photoelectron spectra (XPS) were recorded on a ThermoFisher K-Alpha system using Al Kα radiation with a photon energy of 1486.7 eV The powder samples were immobilized on copper tape before loading into the XPS chamber. Scans were acquired using a 400 μm spot size, 55 eV pass energy, and 0.1 eV/step with charge neutralization. The peak positions were analyzed by calibrating the C 1 s peak at 285 eV The background was subtracted using ThermoAvantage software, applying a *SMART* type background subtraction.

UV/Vis diffuse reflectance spectra (DRS) were recorded on a Lamda 900 spectrophotometer recording the samples' reflectance from an incident wavelength of 250 nm to 600 nm. The bandgap was obtained using the corresponding Tauc plot.

Zeta-potential measurements were executed on a Malvern Zetasizer Nano in a solution of Rhodamine B (12 mg/l_{aq}) and Acid Blue 9 (16 mg/l_{aq}) under experimental conditions of the degradation studies at natural pH with a catalyst concentration of 1 g/l. Prior to the measurement, the sample was stirred for 15 min, dispersed with a Sonotrode (Dr. Hielscher GmbH) for 1 min, followed by 15 min stirring. After equilibrating for 5 min, the sample was measured at 25 °C. For error analysis, each dispersion was measured three times.

Diffuse reflectance infrared Fourier transform spectra (DRIFTS) were recorded on a Thermo Nicolet Nexus IR with the OMNIC software. The sample was heated and measured at 150 °C to reduce adsorbed water's influence. KBr served as a background and was subtracted for each sample.

2.3. Photocatalytic testing

Photocatalytic testing was performed in a 100 ml cylindrical glass container (irradiation surface 11.3 cm^2) with a 30 ml solution of Acid Blue 9 (16 mg/l, 20 μmol/l in deionized water) or Rhodamine B (12 mg/l, 25 μmol/l in deionized water) and 30 mg of catalyst powder. The test was executed in an Atlas SunTest XXL solar simulator equipped with 3 Xenon lamps (45 W/m^2) to ensure homogeneous light distribution. Multiple samples were irradiated simultaneously on a stirring plate (700 rpm) with multiple spots. The powder was dispersed by sonicating the slurry for 10 min. Additionally, the dispersion was stirred in the dark for another 20 min in order to reach the adsorption-desorption equilibrium. 1 ml samples were taken after distinct irradiation times and were then centrifuged, and the supernatant liquid was then analyzed using a UV/Vis spectrometer (Hach-Lange DR5000). The absorption was measured at 629 nm and 554 nm, which are the maxima for Acid Blue 9 and RhB, respectively, from which the dye concentration C was deduced. According to first-order kinetics $\ln(C_0/C_t)$ was plotted vs decomposition time and the slope of the linear regression represents the kinetic constant. Tests with sacrificial agents were executed in the same manner adding 175 μl

(82 mmol/l) of DMSO or 100 μl (82 mmol/l) methanol to the solution.

3. Results and discussion

SiO_2 was added onto the TiO_2 (P25) surface using atomic layer deposition. With this technique, we deposited SiO_2 up to 2.7 wt.% Si

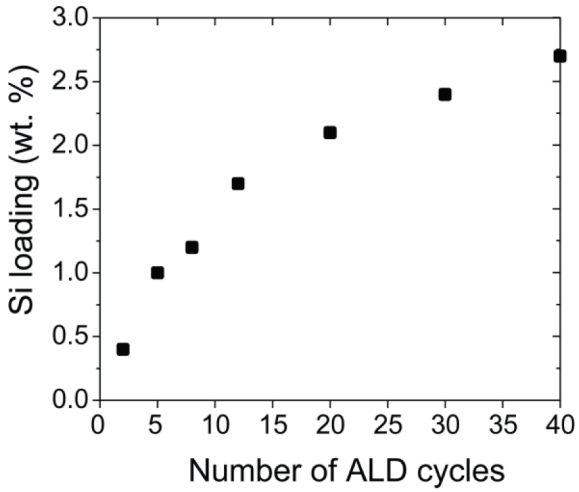

Fig. 1. Loading of Si (wt.%) vs the number of ALD cycles measured by ICP-OES.

(Fig. 1) in a very conformal manner where the Si loading (wt.%) increases with the number of ALD cycles. The higher growth per cycle for a low number of cycles arises from the better reactivity of $SiCl_4$ with the TiO_2 surface. TEM images revealed that the SiO_2 deposition for low-loaded samples might not be complete leaving the TiO_2 surface exposed (Fig. 2a). In a previous study, we have shown that 2 wt.% Si results in a thickness of about 0.7 nm. As the typical Si-O bond has a length of about 0.16 nm [45], the film is less than five bond lengths thick, indicating a high chance of incomplete coverage. The incomplete coverage still allows the oxidation reactions to occur at the TiO_2 surface and is, therefore, beneficial for the overall photocatalytic activity. For higher loaded samples (1.7 wt.% Si and 2.7 wt.% Si), we observe a shell formation around the TiO_2 particles, which increases in film thickness for higher loadings. XPS analysis confirms the deposition of SiO_2 onto TiO_2, which shows peaks at binding energies of 102.68 eV (Si2p) and 458.78 eV ($Ti2p_{3/2}$) and 464.58 eV ($Ti2p_{1/2}$), respectively. Additionally, XPS analysis reveals samples with a low number of $SiCl_4/H_2O$ cycles suffer from contamination with Cl due to an incomplete reaction of $SiCl_2$ with water (Fig. S1). Post-annealing in air at 500 °C converted residual SiO_xCl_{4-2x} into SiO_2 (Fig. S2), eliminating the contamination from the deposition process. Using Rhodamine B (479 g/mol) and AcidBlue 9 (793 g/mol) are large charged molecules which gives the opportunity to evaluate the photocatalyst for two differently charged molecules. Whereas Rhodamine B has a positively charged iminium group and a carbonic acid group (pKa: 3.2) [46], Acid Blue 9 (pKa: 5.8, 6.6) [47] has three sulfonic acid groups giving an overall negatively charged state under natural pH. The photocatalytic degradation of both RhB and AB9 displays a significant improvement with the deposition of SiO_2 onto TiO_2 (Fig. S6, Fig. 3, RhB: 3.5-fold improvement for annealed 1.7 wt.% SiO_2:TiO_2, AB9: 3-fold improvement for annealed 1.7 wt.% SiO_2:TiO_2). Under the used experimental conditions, no degradation of either RhB or AB9 could be observed under artificial solar irradiation in the absence of a catalyst (Fig. S5). Moreover, while the post-treatment affects the photocatalytic activity of TiO_2 insignificantly, it strongly improves the performance of SiO_2:TiO_2. The Cl contamination harms the photocatalytic activity, with especially Acid Blue 9 (AB9) strongly adsorbing on the surface of the low loaded Si samples (Fig. S3). These chlorides in solution may arise from the reaction of water with the residual Cl in SiO_xCl_{4-2x} layer. Chloride contamination in the solution results in a substantial increase in the zeta potential of SiO_2 [48], increasing the adsorption of the negatively charge AB9 molecules. Additionally, chloride ions have been found capable of scavenging holes, leading to a decrease in photocatalytic activity [49, 50], which demonstrates that pure SiO_2 is highly beneficial for photocatalytic improvement. Therefore, for the subsequent experiments, the annealed samples have been used.

Our previous research demonstrated a twofold enhancement for the degradation of Rhodamine B (RhB) with a loading of 1.9 wt.% Si, followed by a total suppression of the photocatalytic activity for higher loadings (> 5 wt.% Si) [17, 42]. As an electric insulator with a bandgap of 9 eV, silicon dioxide is not expected to have photocatalytic properties using the solar spectrum due to insufficient photon energy to generate excited electrons and holes. This lack of charge transport in intrinsic SiO_2 explains the trend towards total suppression of the photocatalytic activity for higher loadings. There, SiO_2 approaches the properties of pure SiO_2 as an intrinsically photocatalytically inactive material. Higher loadings leading to thicker coatings also hinder the pollutants from reaching the active TiO_2 surface and block electron transport from the TiO_2 to the surface [51]. The blocking explains the photocatalytic suppression of thick SiO_2 layers on TiO_2. However, the mechanism behind the photocatalytic enhancement due to an ultrathin SiO_2 layer on TiO_2 particles and the predominant degradation pathways are still lacking

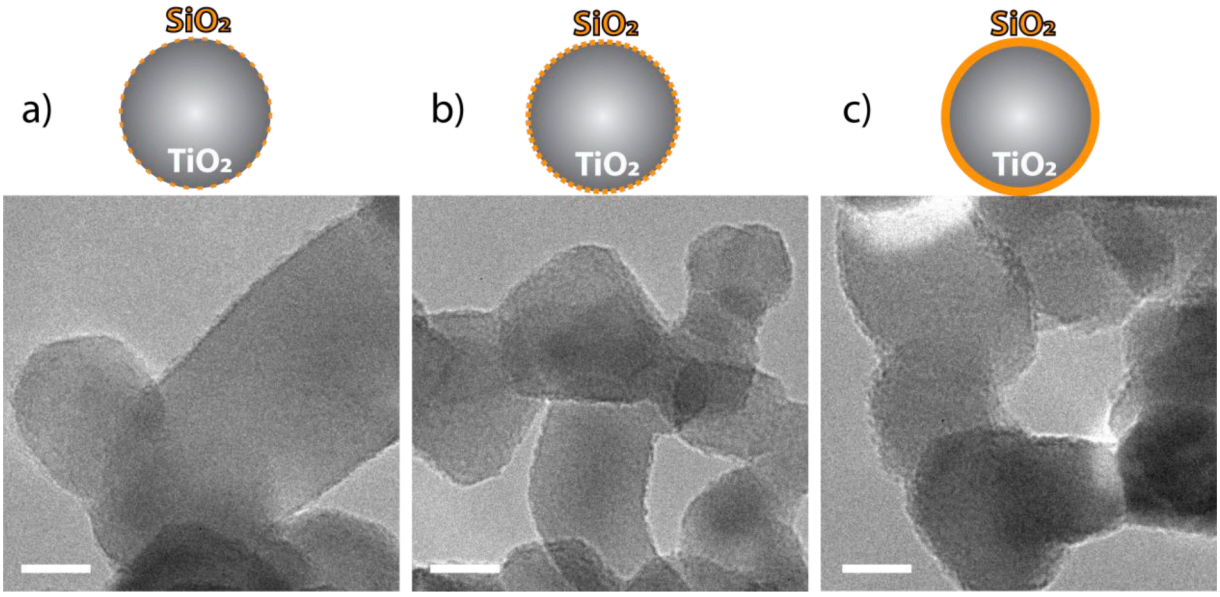

Fig. 2. TEM images of SiO_2 deposition on TiO_2; a) 0.4 wt.% Si, b) 1.7 wt.% Si; c) 2.7 wt.% Si; scalebar represents 10 nm.

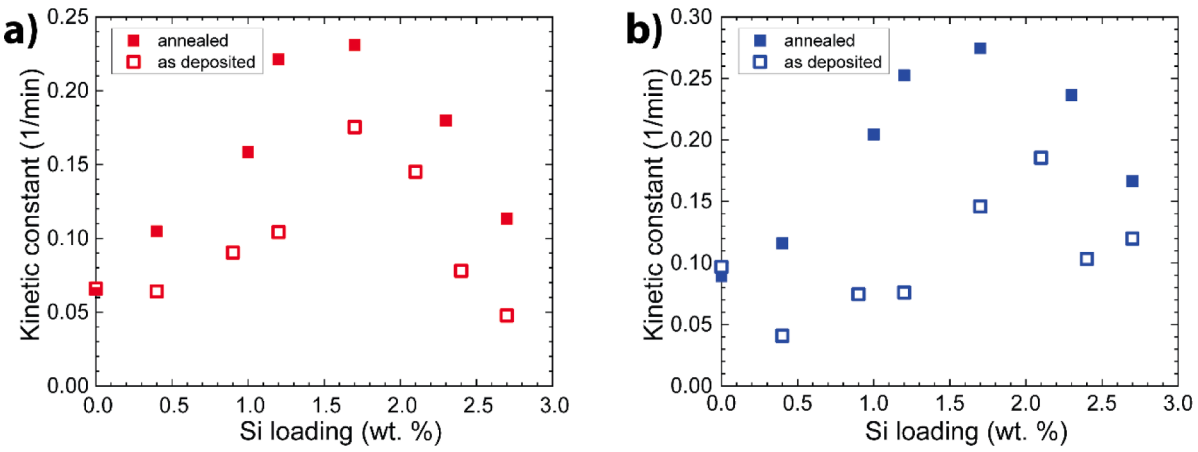

Fig. 3. Kinetic constant for the photocatalytic degradation of a) RhB and b) AB9 using various loadings of Si, open symbols represent the as-deposited samples.

deeper understanding. We will now look at the activity increase for very low loadings using different tools to investigate the photocatalytic mechanism of SiO_2:TiO_2nanoparticles.

It is well known that SiO_2 surfaces have a larger number of acidic OH groups than TiO_2, which will result in a more negative zeta potential: the points of zero charge are about 3 [52] and 6 [53], respectively Fig. 4.a shows the zeta potential for different loadings of SiO_2 on TiO_2. It should be noted that the zeta potential was measured in the dye solutions to imitate the conditions used in the photocatalytic experiments. Uncoated TiO_2 has a slightly positive zeta potential of 0–15 mV, dependent on the dye solution. Upon deposition of SiO_2, the zeta potential decreases to approximately -40 mV the highest SiO_2 loading, clearly indicating both a change in the value and a change from positive to negative values. This is a result of the difference of the isoelectric point (IEP) of SiO_2 (IEP = 3) versus TiO_2 (IEP = 6) [26, 54]. The zeta potential of the powders dispersed in the solution of AB9 is generally more negative than in a solution of RhB (Fig. 4a), indicating that AB9, as a negatively charged dye, adsorbs strongly on the intrinsically positively charged TiO_2 surface, decreasing the effective positive charge. The change of zeta-potential upon deposition of SiO_2 on TiO_2 particles is expected to lead to a difference in the adsorption behavior of RhB – a positively charged dye. Upon deposition of SiO_2, as the particle surface charge becomes negative the adsorption-desorption equilibrium of AB9 (negatively charged) trends to negligible adsorption, whereas for RhB (positively charged), an increase of adsorption and decreased concentration is observed for higher loadings (Fig. 4b).

Although negligible adsorption of AB9 on the surface of SiO_2 (Fig. 4b), we still can observe an improvement in the photocatalytic activity (~2.5 times enhancement at 1.7 wt.% Si versus uncoated TiO_2; Fig. 3b). The improved activity demonstrates that reactants' eventual adsorption plays an insignificant role in the photocatalytic activity of SiO_2:TiO_2.

Surface OH groups have an important role in the photocatalytic activity of TiO_2 [55]. DRIFTS analysis provides insight into the quantity and type of OH groups on the surface. The number of acidic surface OH groups on the SiO_2 surface (3740 cm^{-1}) increases with the Si loading reaching a plateau at 1.7 wt.% Si. While for 0.4 wt.% Si, the Ti-OH peaks (3600 – 3700 cm^{-1}) are still clearly visible, indicating only partial coverage of SiO_2 on TiO_2, the Ti–OH peaks become less pronounced with increasing Si loading (Fig 5). These findings are also in agreement with the TEM micrographs, which demonstrate a partial coverage of SiO_2 on the TiO_2 surface for 0.4 wt.% Si trending towards encapsulation for higher loadings (>1.7 wt.% Si). The more acidic OH groups on the silica surface can promote the generation of OH* radicals [22, 56]. The trend in the number of OH groups strongly correlates with the improvement of the photocatalytic activity for low loadings until 1.7 wt.% Si demonstrating the influence of OH groups on the photocatalytic activity. Moreover, the stagnant number of OH groups for higher Si loadings combined with the insulating properties would result in the observed optimal loading for SiO_2 on TiO_2 for the photocatalytic degradation.

In order to check the reaction pathways scavenging agents can be utilized to block specific pathways to find which contribution dominates in the photocatalytic degradation. Organic pollutants are generally degraded via three pathways [49, 57]: 1) direct oxidation by reaction

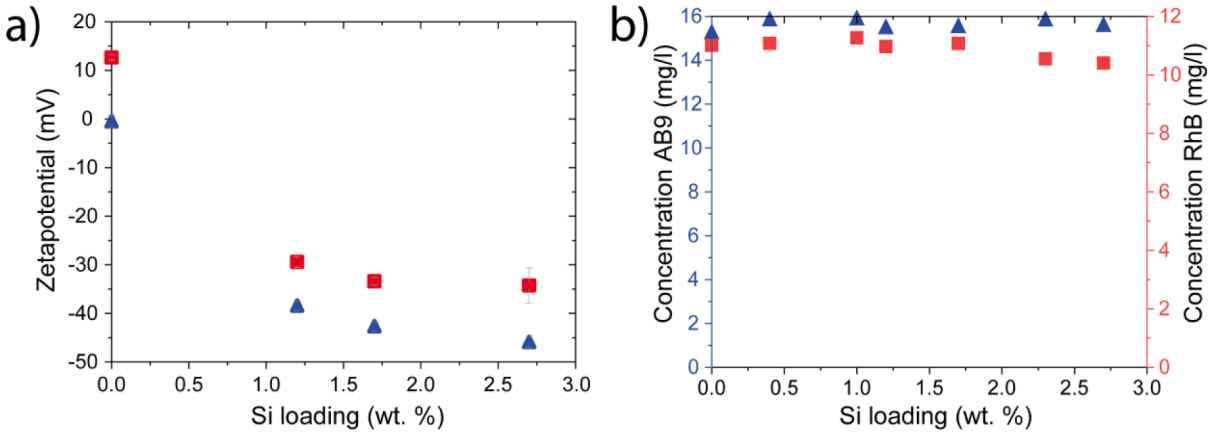

Fig. 4. a) Zeta potential vs. Si loading (blue data points represent zeta potential in AB9 solution and red data points in RhB solution) b) Remaining concentration of AB9 (blue triangles) and RhB (red squares) after reaching the adsorption-desorption equilibrium. The initial concentration for AB9 and RhB was 16 mg/l and 12 mg/l, respectively.

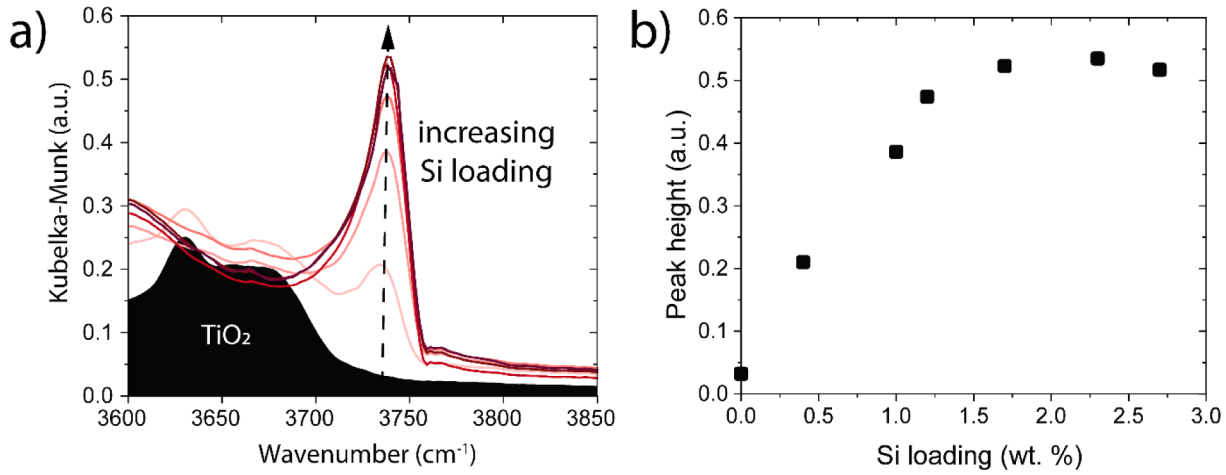

Fig. 5. a) DRIFTS spectrum of different loadings of SiO_2 on TiO_2 in the characteristic range for surface OH groups, b) Peak height of Si-OH signal in DRIFTS spectra for samples with various Si loading.

with a hole, and 2) decomposition by reaction with OH* radicals, generated via h^+_{VB}, or 3) using the excited electrons in the conduction band to facilitate the O_2 reduction followed by OH* radical formation (Fig. 6b). DMSO is often used as a scavenging agent for hydroxyl radicals [9, 58–60] The addition of DMSO in a large excess (scavenger/pollutant) to the catalyst suspension should, in case of an OH* radical mechanism, result in a strong inhibition of the photocatalytic degradation. In case the OH radicals play a minor role, the photocatalytic activity should only be minorly affected. Surprisingly, DMSO promotes the photocatalytic degradation of both AB9 and RhB when added to the TiO_2 suspension. Other studies in the field of biology report DMSO as an acceptor for electrons to be reduced to dimethylsulfide. [61, 62]. Therefore, DMSO may not only able to scavenge OH* radicals but also react with the CB electrons. In the case of TiO_2, this would thus result in the observed increase in the photocatalytic activity since the scavenging of the CB electrons will lead to suppression of charge recombination, allowing more VB holes to react with the pollutant directly. The results lead to the conclusion that by adding DMSO, the degradation of the pollutant only can be achieved by direct oxidation, which also indicates that degradation via OH* radicals, on the other hand, is not very effective for TiO_2. A detailed comparison of the experimental conditions with other studies on TiO_2 remains challenging due to incomplete information on the process conditions and scavenger concentration in many publications. When adding MeOH – a hole scavenger [63, 64], blocking all degradation pathways originating from the valence band – in both cases (AB9 and RhB) for TiO_2, the photocatalytic activity drops. In the case of RhB, degradation is strongly hindered, which demonstrates that MeOH blocks the degradation pathways via the VB but also that the degradation pathway via the CB is not a dominant pathway for dye degradation using TiO_2. These results suggest that the primary contributing mechanism is direct oxidation of the pollutant, which advocates that pollutants' adsorption is an essential step for the photocatalytic degradation using TiO_2. For the degradation of AB9, MeOH decreases the activity only slightly. AB9 and MeOH compete for the adsorption on the surface because of the negative charge of AB9, which is attracted by the positively charged TiO_2 surface. This leads to the degradation of AB9, whereas RhB (with its positive charge, negligibly adsorbed on the TiO_2 surface) seems to remain unreacted. Although these results indicate that direct oxidation dominates the degradation pathway of dyes, the degradation of RhB suggests that direct oxidation is not the exclusive mechanism, and the generation of ROS (i.e. OH*, O_2^{-}*) is still occurring, yet less pronounced.

In the case of SiO_2:TiO_2, DMSO strongly reduces the photocatalytic activity. As stated earlier, DMSO blocks not only the degradation via OH* radicals generated via the VB but may also affect the CB pathways by scavenging the CB electrons. Therefore, only the degradation via

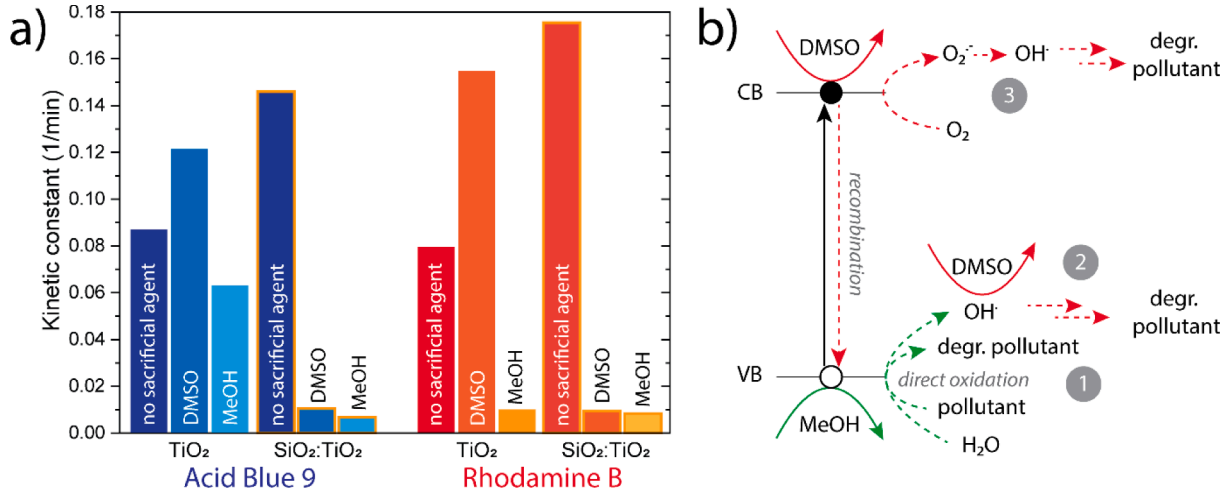

Fig. 6. a) Kinetic constants for photocatalytic degradation of RhB or AB9 using DMSO (as CB electron scavenger and OH* radical scavenger) or MeOH (as hole scavenger) for TiO_2 and SiO2: TiO_2 (1.7 wt.% Si). b) Schematic reaction pathways showing the influence of sacrificial agents DMSO and MeOH, dashed lines represent the reaction pathways that are prevented by the addition of sacrificial agents.

direct oxidation would still be accessible. However, very little activity is observed, which poses that direct oxidation is not very pronounced for dye degradation using SiO_2:TiO_2. Adding MeOH decreases the activity to the same extent as DMSO. This implies that also CB pathways are not the predominant degradation pathways since all VB pathways are blocked for dye degradation. These findings suggest that the OH* radicals generated via the VB pathway on the SiO_2 surface are the dominant species for dye degradation using SiO_2: TiO_2. The OH* radicals will be formed on the SiO_2 surface, diffusing into the solution [56].

Diffuse reflection measurements of the catalyst materials only showed a negligible effect of the SiO_2 coating on the absorption properties of the coated catalysts due to the fact that the SiO_2 layer is ultrathin (Fig. S4). Previous research proposed that thin layers of SiO_2, despite the insulating properties of pure SiO_2, not only allow the hole transfer to the surface by a tunneling effect due to a very thin coating of SiO_2 or likely incomplete layer but also improve the charge separation due to the formation of a space charge layer as a consequence of Si-O-Ti interlinkages at the SiO_2-TiO_2 interface [39, 65, 66]. The loading with low amounts of SiO_2 gives rise to incomplete coverage of the TiO_2 particles leaving the TiO_2 surface exposed. Therefore, the excited electrons will be able to react on the accessible TiO_2 surface impeding electron-hole recombination [30]. This has also been confirmed by Guo et al. who found an intensity decrease in the photoluminescence signal upon deposition of SiO_2 on TiO_2 as a consequence of electron-hole recombination [42]. Overall, the efficient charge separation followed by electron consumption at the TiO_2 surface and simultaneous hole transfer to the SiO_2 surface inducing the subsequent reaction with the more acidic Si–OH groups will result in the increased formation of OH* radicals. However, not only is the activity increased but also the mechanism has changed compared to TiO_2, i.e., low amounts of SiO_2 on TiO_2 change the contribution of the different pathways from direct oxidation (TiO_2) to degradation via OH* radicals (SiO_2:TiO_2). Simultaneous degradation of both types f dye molecules will further elucidate this conclusion.

Testing the photocatalytic behavior of both materials – TiO_2 and SiO_2:TiO_2 – by the simultaneous degradation of AB9 and RhB gives insight into the selectivity and degradation behavior towards these pollutants.

Following the color of the reaction solution by eye already indicates different degradation kinetics (Fig. 7a, b). While for TiO_2, the red color (RhB) remains longer in solution, SiO_2:TiO_2 maintains the blue color (AB9) for longer, indicating a quicker degradation of AB9 and RhB for TiO_2 and SiO_2:TiO_2, respectively. Moreover, SiO_2:TiO_2 decolorizes the solution overall faster than uncoated TiO_2, proving the superiority of SiO_2:TiO_2 over uncoated TiO_2. In detail, TiO_2 degrades AB9 faster than RhB showing first-order kinetics similar to the degradation of only AB9 in the solution. Additionally, the mixture of AB9 and RhB results in stronger and preferential adsorption of AB9 on the surface of TiO_2. On the other hand, the degradation of RhB is obstructed in the beginning when the concentration of AB9 is still high, only accelerating starting from 30 min when a low concentration of AB9 remains in the solution. This obstruction changes the kinetics of the degradation of RhB from 1st order kinetics, over the whole range of reaction time, to two distinct time regimes. The first regime from 0 to 30 min indicates limited adsorption of RhB due to the competition with AB9 (0–30 min). In the following regime (30–80 min), the low AB9 concertation has only a limited interference with the degradation mechanism of RhB. Direct dye oxidation dominates the degradation, where negatively charged AB9 adsorbed on the positive TiO_2 surface will impede RhB from getting access to reactive oxygen species and subsequently being degraded. Only after the concentration of AB9 on the surface has decreased sufficiently, RhB may reach the proximity of the TiO_2 to be attacked by

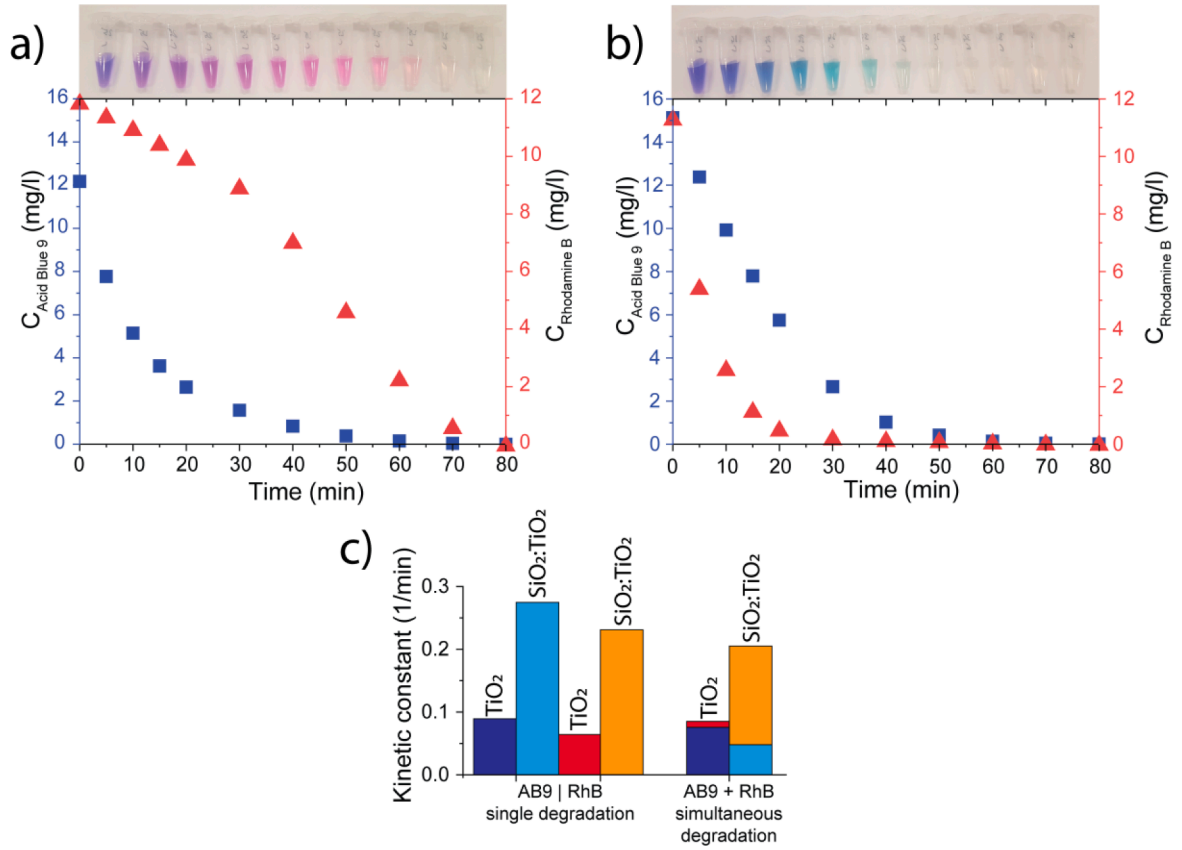

Fig. 7. Simultaneous degradation of AB9 (blue squares) and RhB (red triangles) using a) TiO_2 and b) SiO2:TiO_2 (1.7 wt.% Si); c) first-order kinetic constants (0–20 min) for degradation of single compounds and simultaneous degradation of AB9 and RhB, the kinetic constants for simultaneous degradation are stacked.

radical species. ROS may diffuse to the RhB molecules in solution, additionally demonstrating the importance of adsorption on the surface, advocating that the direct oxidation pathway is prevalent for TiO_2. The similar degradation speed for AB9 in the single degradation and combined degradation substantiates this pathway (Fig. 7c, Table 1).

For SiO_2:TiO_2, in addition to faster degradation of RhB over AB9 in the dye mixture, the first-order reaction mechanism remains valid for both individual dye degradations. With the positive charge, RhB prevails over AB9 for the competitive attraction to the negatively charged SiO_2 surface where the reactive oxygen species are formed, which explains the faster degradation of RhB (50 min) versus AB9 (70 min) as displayed in Fig. 7b. In contrast to TiO_2, both dyes are degraded truly simultaneously in first-order kinetics. Comparing the kinetic constants with only a single dye in solution, the degradation proceeds overall slower. However, the sum of the kinetic constants gives about equal values for individual degradation (Table 1). This indicates that both dyes are reached by degradation species simultaneously. This insight is in agreement with our previous finding that for

SiO_2: TiO_2, OH* radicals are the predominant degradation pathway rather than direct oxidation on the surface. OH* radicals, generated on the surface, can diffuse to a certain extent into the solution, making the pollutant's direct adsorption less relevant for photocatalytic degradation. Considering this mechanism, both individual kinetic constants for the combined degradation should add up to the kinetic constant obtained from the single dye degradation. However, the combined kinetic constant is slightly lower than the kinetic constant of the single dyes. This behavior is already well observed in the literature that the kinetic constant decreases due to mass transport limitations in high pollutant concentrations [2, 49]. From the studies with sacrificial agents and the simultaneous degradation of two dyes, we can summarize that the TiO_2 main but not exclusive mechanism refers to direct oxidation for degrading organic pollutants, which can be concluded by the preferred degradation of the adsorbed pollutant. On the other hand, the simultaneous degradation of both dyes proves the preferred degradation via OH* radicals for SiO_2:TiO_2 where direct contact with the surface is less important. Generated OH* radicals will diffuse into the solution to oxidize molecules that are not directly adsorbed on the surface. Therefore, apart from the general improvement of SiO_2:TiO_2 over TiO_2 due to the easier OH* radical generation from Si–OH groups, SiO_2:TiO_2 degrades organic dyes less selectively. Although this lower selectivity might be disadvantageous for degradation of a defined effluent from a production site, the goal to clean water from an undefined water source requires unselective degradation of all organic matter to obtain good water quality.

The investigation of other materials for ultrathin coatings onto TiO_2 that are typically easily achievable with ALD to precisely tune its surface properties could lead to further development for cheaper photocatalysts. However, for Al_2O_3, we found previously that even sub-nanometer coatings on TiO_2 suppress the photocatalytic activity strongly, emphasizing the special properties of SiO_2 [67]. Clarifying the photocatalytic mechanism for SiO_2:TiO_2 and applying this knowledge on the different degradation mechanisms opens doors to further developments where specific properties can be fine-tuned in catalyst development. Several modifications e.g. with atomic layer deposition with different materials, might improve individual pathways for radical generation and manufacture, therefore, an overall better photocatalyst.

4. Conclusion

We have shown that deposition of a low amount of SiO_2 onto TiO_2, which only results in partial coverage of the TiO_2 surface, can enhance the photocatalytic activity for the degradation of dyes independent of the charge of the pollutant. This indicates that the change of the surface charge by the deposition of SiO_2 on TiO_2 only has limited influence on the improved photocatalytic activity. The surface charge of SiO_2-coated TiO_2 (negative) versus uncoated TiO_2 (positive) changes only the preference for which pollutant will be degraded first when both are degraded simultaneously. For independent dye degradation experiments, SiO_2:TiO_2 shows superior photocatalytic activity, which can be ascribed to the more acidic OH groups on the surface introduced by the SiO_2 coating and the enhanced electron-hole separation due to the Ti–O–Si linkages at the TiO_2–SiO_2 interface as proposed in the literature. Using DMSO and MeOH as sacrificial agents, we have shown the difference in photocatalytic behavior of TiO_2 and SiO_2:TiO_2. From these experiments, it can be concluded that TiO_2 prevalently degrades organic pollutants via direct oxidation by reaction with holes, whereas SiO_2:TiO_2 mainly enhances the OH* radical formation from reaction with holes, which is then responsible for pollutant degradation.

Table 1
Kinetic constants for the degradation of AB9, RhB (single), and RhB+AB9 (combined) using TiO_2 and SiO_2:TiO_2 (1.7 wt.% Si). According to first-order kinetics, the kinetic constants were fitted from 0 to 20 min.

Kinetic constant (min^{-1})	AB9*single*	AB9*simultaneous*	RhB*single*	RhB*simultaneous*
TiO_2	0.087 ± 0.001	0.079 ± 0.002	0.066 ± 0.001	0.009 ± 0.001
SiO_2:TiO_2	0.263 ± 0.006	0.046 ± 0.001	0.230 ± 0.003	0.154 ± 0.002

Declaration of Competing Interest

J.R. van Ommen has a financial interest in Delft IMP.

Acknowledgments

We would like to acknowledge Bart van der Linden from the Catalysis Engineering group for support on the DRIFTS measurements and the annealing procedure, Ruben Abellon from the Optoelectronic materials group for supporting the UV/Vis DRS experiments, Baukje Terpstra from the Applied Radiation & Isotopes group for ICP-OES measurements and Jan Köser from the University of Bremen for the kind support in the zeta potential measurements. Moreover, authors would like to acknowledge Guido Mul and Robert Bruninghoff for the helpful scientific discussions. This research is supported by the TU Delft | Global Initiative, a program of the Delft University of Technology to boost Science and Technology for Global Development.

Supplementary materials

Supplementary material associated with this article can be found, in the online version, at doi:10.1016/j.ceja.2022.100288.

References

[1] A. Fujishima, K. Honda, Electrochemical photolysis of water at a semiconductor electrode, Nature 238 (1972) 37–38.
[2] K.M. Reza, A.S.W. Kurny, F. Gulshan, Parameters affecting the photocatalytic degradation of dyes using TiO_2: a review, Appl. Water Sci. 7 (2015) 1569–1578.
[3] O. Carp, C.L. Huisman, A. Reller, Photoinduced reactivity of titanium dioxide, Prog. Solid State Chem. 32 (2004) 33–177.
[4] J. Trawiński, R. Skibiński, Rapid degradation of clozapine by heterogeneous photocatalysis. Comparison with direct photolysis, kinetics, identification of transformation products and scavenger study, Sci. Total Environ. 665 (2019) 557–567.
[5] A. Fujishima, T.N. Rao, D.A. Tryk, Titanium dioxide photocatalysis, J. Photochem. Photobiol. C 1 (2000) 1–21.
[6] Y. Nosaka, A. Nosaka, Understanding hydroxyl radical (•OH) generation processes in photocatalysis, ACS Energy Lett. 1 (2016) 356–359.
[7] J. Zhang, Y. Nosaka, Mechanism of the OH radical generation in photocatalysis with TiO_2 of different crystalline types, J. Phys. Chem. C 118 (2014) 10824–10832.
[8] I. Levchuk, C. Guillard, F. Dappozze, S. Parola, D. Leonard, M. Sillanpaa, Photocatalytic activity of TiO_2 films immobilized on aluminum foam by atomic layer deposition technique, J. Photochem. Photobiol. A-Chem. 328 (2016) 16–23.
[9] X.H. Lin, Y. Miao, S.F.Y. Li, Location of photocatalytic oxidation processes on anatase titanium dioxide, Catal. Sci. Technol. 7 (2017) 441–451.

[10] S. Mortazavian, A. Saber, D.E. James, Optimization of photocatalytic degradation of acid blue 113 and acid red 88 textile dyes in a UV-C/TiO_2 suspension system: application of response surface methodology (RSM), Catalysts 9 (2019) 360.

[11] M. Motegh, J. Cen, P.W. Appel, J.R. van Ommen, M.T. Kreutzer, Photocatalytic-reactor efficiencies and simplified expressions to assess their relevance in kinetic experiments, Chem. Eng. J. 207-208 (2012) 607–615.

[12] S.J.A. Moniz, J. Tang, Charge transfer and photocatalytic activity in CuO/TiO_2 nanoparticle heterojunctions synthesised through a rapid, one-pot, microwave solvothermal route, ChemCatChem 7 (2015) 1659–1667.

[13] O. Nasr, O. Mohamed, A.-.S. Al-Shirbini, A.-.M. Abdel-Wahab, Photocatalytic degradation of acetaminophen over Ag, Au and Pt loaded TiO_2 using solar light, J. Photochem. Photobiol. A 374 (2019) 185–193.

[14] Y.C. Liang, C.C. Wang, C.C. Kei, Y.C. Hsueh, W.H. Cho, T.P. Perng, Photocatalysis of Ag-loaded TiO_2 nanotube arrays formed by atomic layer deposition, J. Phys. Chem. C 115 (2011) 9498–9502.

[15] S.J.A. Moniz, S.A. Shevlin, X. An, Z.-.X. Guo, J. Tang, Fe_2O_3–TiO_2 nanocomposites for enhanced charge separation and photocatalytic activity, Chem. – Eur. J. 20 (2014) 15571–15579.

[16] A.S. Ganeshraja, K. Rajkumar, K. Zhu, X. Li, S. Thirumurugan, W. Xu, J. Zhang, M. Yang, K. Anbalagan, J. Wang, Facile synthesis of iron oxide coupled and doped titania nanocomposites: tuning of physicochemical and photocatalytic properties, RSC Adv. 6 (2016) 72791–72802.

[17] D. Benz, Modifying TiO_2 Nanoparticles by Atomic Layer Deposition for Enhanced Photocatalytic Water Purification, Delft University of Technology, Delft, 2020.

[18] S. Dong, J. Feng, M. Fan, Y. Pi, L. Hu, X. Han, M. Liu, J. Sun, J. Sun, Recent developments in heterogeneous photocatalytic water treatment using visible light-responsive photocatalysts: a review, RSC Adv. 5 (2015) 14610–14630.

[19] M.R. Hoffmann, S.T. Martin, W. Choi, D.W. Bahnemann, Environmental applications of semiconductor photocatalysis, Chem. Rev. 95 (1995) 69–96.

[20] K. Lee, H. Yoon, C. Ahn, J. Park, S. Jeon, Strategies to improve the photocatalytic activity of TiO_2: 3D nanostructuring and heterostructuring with graphitic carbon nanomaterials, Nanoscale 11 (2019) 7025–7040.

[21] U.I. Gaya, Origin of the Activity of Semiconductor Photocatalysts, Heterogeneous Photocatalysis Using Inorganic Semiconductor Solids, Springer Netherlands, Dordrecht, 2014, pp. 91–135.

[22] A. Romero-Morán, J.L. Sánchez-Salas, J. Molina-Reyes, Influence of selected reactive oxygen species on the photocatalytic activity of TiO_2/SiO_2 composite coatings processed at low temperature, Appl. Catal. B 291 (2021) 119685.

[23] D. Benz, Y.-N.T. Nguyen, T.-L.T. Le, T.-H.T. Le, V.-.T. Le, J.R. van Ommen, H. Van Bui, Controlled growth of ultrasmall Cu_2O clusters on TiO_2 nanoparticles by atmospheric-pressure atomic layer deposition for enhanced photocatalytic activity, Nanotechnology 32 (2021) 425601.

[24] S. Ullah, E.P. Ferreira-Neto, A.A. Pasa, C.C.J. Alcântara, J.J.S. Acuña, S.A. Bilmes, M.L. Martínez Ricci, R. Landers, T.Z. Fermino, U.P. Rodrigues-Filho, Enhanced photocatalytic properties of core@shell SiO_2@TiO_2 nanoparticles, Appl. Catal. B 179 (2015) 333–343.

[25] P.A. Williams, C.P. Ireland, P.J. King, P.A. Chater, P. Boldrin, R.G. Palgrave, J. B. Claridge, J.R. Darwent, P.R. Chalker, M.J. Rosseinsky, Atomic layer deposition of anatase TiO_2 coating on silica particles: growth, characterization and evaluation as photocatalysts for methyl orange degradation and hydrogen production, J. Mater. Chem. 22 (2012) 20203–20209.

[26] B. Ekka, M.K. Sahu, R.K. Patel, P. Dash, Titania coated silica nanocomposite prepared via encapsulation method for the degradation of Safranin-O dye from aqueous solution: optimization using statistical design, Water Resour. Ind. 22 (2016) 100071.

[27] K. Risa, S. Naoki, O. Makoto, Controlled photocatalytic ability of titanium dioxide particle by coating with nanoporous silica, Chem. Lett. 37 (2008) 76–77.

[28] B. Kim, I. Yang, J.C. Jung, T.S. Lee, B. Yeom, Titania nanoparticle-loaded mesoporous silica synthesized through layer-by-layer assembly for the photodegradation of sodium dodecylbenzenesulfonate, Appl. Surf. Sci. 490 (2019) 38–46.

[29] I.S. Grover, R.C. Prajapat, S. Singh, B. Pal, SiO_2-coated pure anatase TiO_2 catalysts for enhanced photo-oxidation of naphthalene and anthracene, Particuology 34 (2017) 156–161.

[30] A. Giesriegl, J. Blaschke, S. Naghdi, D. Eder, Rate-limiting steps of dye degradation over titania-silica core-shell photocatalysts, Catalysts 9 (2019).

[31] M. Nussbaum, Y. Paz, Ultra-thin SiO_2 layers on TiO_2: improved photocatalysis by enhancing products' desorption, Phys. Chem. Chem. Phys. 14 (2012) 3392–3399.

[32] J. Oguma, Y. Kakuma, M. Nishikawa, Y. Nosaka, Effects of silica-coating on the photoinduced hole formation and decomposition activity of titanium dioxide photocatalysts under UV irradiation, Catal. Letters 142 (2012) 1474–1481.

[33] Y. Ide, Y. Koike, M. Ogawa, Molecular selective photocatalysis by TiO_2/nanoporous silica core/shell particulates, J. Colloid Interface Sci. 358 (2011) 245–251.

[34] Y. Ren, W. Li, Z. Cao, Y. Jiao, J. Xu, P. Liu, S. Li, X. Li, Robust TiO_2 nanorods-SiO_2 core-shell coating with high-performance self-cleaning properties under visible light, Appl. Surf. Sci. 509 (2020) 145377.

[35] D. Wang, Z. Geng, P. Hou, P. Yang, X. Cheng, S. Huang, Rhodamine B removal of TiO_2@SiO_2 core-shell nanocomposites coated to buildings, Cryst. 10 (2020) 80.

[36] Y. Yu, W. Xu, J. Fang, D. Chen, T. Pan, W. Feng, Y. Liang, Z. Fang, Soft-template assisted construction of superstructure TiO_2/SiO_2/g-C_3N_4 hybrid as efficient visible-light photocatalysts to degrade berberine in seawater via an adsorption-photocatalysis synergy and mechanism insight, Appl. Catal. B 268 (2020) 118751.

[37] K. Siwińska-Ciesielczyk, D. Świgoń, P. Rychtowski, D. Moszyński, A. Zgoła-Grześkowiak, T. Jesionowski, The performance of multicomponent oxide systems based on TiO_2, ZrO_2 and SiO_2 in the photocatalytic degradation of Rhodamine B: mechanism and kinetic studies, Colloids Surf. A 586 (2020) 124272.

[38] C. Anderson, A.J. Bard, An improved photocatalyst of TiO_2/SiO_2 prepared by a sol-gel synthesis, J. Phys. Chem. 99 (1995) 9882–9885.

[39] L. Yuan, C. Han, M. Pagliaro, Y.-.J. Xu, Origin of enhancing the photocatalytic performance of TiO_2 for artificial photoreduction of CO_2 through a SiO_2 coating strategy, J. Phys. Chem. C 120 (2016) 265–273.

[40] Y. Gong, D.P. Wang, R. Wu, S. Gazi, H.S. Soo, T. Sritharan, Z. Chen, New insights into the photocatalytic activity of 3-D core–shell P25@silica nanocomposites: impact of mesoporous coating, Dalton Trans. 46 (2017) 4994–5002.

[41] S. Hu, F. Li, Z. Fan, Preparation of SiO_2-coated TiO_2 composite materials with enhanced photocatalytic activity under UV light, Bull. Korean Chem. Soc. 33 (2012) 1895–1899.

[42] J. Guo, D. Benz, T.-.T. Doan Nguyen, P.-.H. Nguyen, T.-.L. Thi Le, H.-.H. Nguyen, D. La Zara, B. Liang, H.T. Hintzen, J.R. van Ommen, H. Van Bui, Tuning the photocatalytic activity of TiO_2 nanoparticles by ultrathin SiO_2 films grown by low-temperature atmospheric pressure atomic layer deposition, Appl. Surf. Sci. 530 (2020) 147244.

[43] R. Beetstra, U. Lafont, J. Nijenhuis, E.M. Kelder, J.R. van Ommen, Atmospheric pressure process for coating particles using atomic layer deposition, Chem. Vap. Deposition 15 (2009) 227–233.

[44] J.R. van Ommen, A. Goulas, Atomic layer deposition on particulate materials, Mater. Today Chem. 14 (2019), 100183.

[45] W. Baur, Silicon-oxygen bond lengths, bridging angles Si-O-Si and synthetic low tridymite, Acta Crystallogr. Section B 33 (1977) 2615–2619.

[46] M. Flury, N.N. Wai, Dyes as tracers for vadose zone hydrology, Rev. Geophys. 41 (2003).

[47] M. Flury, H. Flühler, Tracer characteristics of brilliant blue FCF, Soil Sci. Soc. Am. J. 59 (1995) 22–27.

[48] M. Kosmulski, Positive electrokinetic charge of silica in the presence of chlorides, J. Colloid Interface Sci. 208 (1998) 543–545.

[49] S. Ahmed, M.G. Rasul, W.N. Martens, R. Brown, M.A. Hashib, Advances in heterogeneous photocatalytic degradation of phenols and dyes in wastewater: a review, Water Air Soil Pollut. 215 (2010) 3–29.

[50] M. Sökmen, A. Özkan, Decolourising textile wastewater with modified titania: the effects of inorganic anions on the photocatalysis, J. Photochem. Photobiol. A 147 (2002) 77–81.

[51] A.M. El-Toni, S. Yin, T. Sato, Control of silica shell thickness and microporosity of titania-silica core-shell type nanoparticles to depress the photocatalytic activity of titania, J. Colloid Interface Sci. 300 (2006) 123–130.

[52] J.P. Cloarec, C. Chevalier, J. Genest, J. Beauvais, H. Chamas, Y. Chevolot, T. Baron, A. Souifi, pH driven addressing of silicon nanowires onto Si_3N_4/SiO_2 micro-patterned surfaces, Nanotechnology 27 (2016) 295602.

[53] M. Zeng, Influence of TiO_2 surface properties on water pollution treatment and photocatalytic activity, Bull. Korean Chem. Soc. 34 (2013) 953–956.

[54] G. Konecoglu, T. Safak, Y. Kalpakli, M. Akgun, Photocatalytic degradation of textile dye CI basic yellow 28 wastewater by Degussa P25 based TiO_2, Adv. Environ. Res. 4 (2015) 25–38.

[55] M.E. Simonsen, Z. Li, E.G. Søgaard, Influence of the OH groups on the photocatalytic activity and photoinduced hydrophilicity of microwave assisted sol–gel TiO_2 film, Appl. Surf. Sci. 255 (2009) 8054–8062.

[56] J. Narayanasamy, J.D. Kubicki, Mechanism of hydroxyl radical generation from a silica surface: molecular orbital calculations, J. Phys. Chem. B 109 (2005) 21796–21807.

[57] U.I. Gaya, Principles of Heterogeneous Photocatalysis, Heterogeneous Photocatalysis Using Inorganic Semiconductor Solids, Springer Netherlands, Dordrecht, 2014, pp. 1–41.

[58] O.F. Lopes, K.T.G. Carvalho, G.K. Macedo, V.R. de Mendonça, W. Avansi, C. Ribeiro, Synthesis of $BiVO_4$ via oxidant peroxo-method: insights into the photocatalytic performance and degradation mechanism of pollutants, New J. Chem. 39 (2015) 6231–6237.

[59] R.V. Panganamala, H.M. Sharma, R.E. Heikkila, J.C. Geer, D.G. Cornwell, Role of hydroxyl radical scavengers dimethyl sulfoxide, alcohols and methional in the inhibition of prostaglandin biosynthesis, Prostaglandins 11 (1976) 599–607.

[60] Y. Yoshimura, T. Inomata, H. Nakazawa, H. Kubo, F. Yamaguchi, T. Ariga, Evaluation of free radical scavenging activities of antioxidants with an H_2O_2/NaOH/DMSO system by electron spin resonance, J. Agric. Food Chem. 47 (1999) 4653–4656.

[61] S.H. Zinder, T.D. Brock, Dimethyl sulfoxide as an electron acceptor for anaerobic growth, Arch. Microbiol. 116 (1978) 35–40.

[62] A.S. Beliaev, D.M. Klingeman, J.A. Klappenbach, L. Wu, M.F. Romine, J.M. Tiedje, K.H. Nealson, J.K. Fredrickson, J. Zhou, Global transcriptome analysis of Shewanella oneidensis MR-1 exposed to different terminal electron acceptors, J. Bacteriol. 187 (2005) 7138–7145.

[63] T. Puangpetch, T. Sreethawong, S. Yoshikawa, S. Chavadej, Hydrogen production from photocatalytic water splitting over mesoporous-assembled $SrTiO_3$ nanocrystal-based photocatalysts, J. Mol. Catal. A Chem. 312 (2009) 97–106.

[64] W. Jones, D.J. Martin, A. Caravaca, A.M. Beale, M. Bowker, T. Maschmeyer, G. Hartley, A. Masters, A comparison of photocatalytic reforming reactions of methanol and triethanolamine with Pd supported on titania and graphitic carbon nitride, Appl. Catal. B 240 (2019) 373–379.

[65] K. Miyashita, S.-i. Kuroda, T. Sumita, T. Ubukata, H. Kubota, Spectrum response of the vacuum-deposited SiO_2/TiO_2 multilyaer film with improved photo-catalytic activity, J. Mater. Sci. Lett. 20 (2001) 2137–2140.
[66] K. Guan, H. Xu, B.J. Lu, Hydrophilic property of SiO_2-TiO_2 overlayer films and TiO_2/SiO_2 mixing films, Trans. Nonferrous Metals Soc. China (English Edition) 14 (2004) 251–254.
[67] J. Guo, H. Van Bui, D. Valdesueiro, S. Yuan, B. Liang, J.R. van Ommen, Suppressing the photocatalytic activity of TiO_2 nanoparticles by extremely thin Al_2O_3 films grown by gas-phase deposition at ambient conditions, Nanomaterials 8 (2018) 61.